FLEXFLOIL SHAPE ADAPTIVE CONTROL SURFACES—FLIGHT TEST AND NUMERICAL RESULTS

Sridhar Kota*, Joaquim R. R. A. Martins**
***FlexSys Inc. , **University of Michigan**

Keywords: *FlexFoil, adaptive compliant trailing edge, flight testing, aerostructural optimization*

Abstract

The U.S Air Force and NASA recently concluded a series of flight tests, including high speed ($M = 0.85$) and acoustic tests of a Gulfstream III business jet retrofitted with shape adaptive trailing edge control surfaces under the Adaptive Compliant Trailing Edge (ACTE) program. The long-sought goal of practical, seamless, shape-changing control surface technologies has been realized by the ACTE program in which the high-lift flaps of the Gulfstream III test aircraft were replaced with 23 ft spanwise FlexFoil™ variable geometry control surfaces on each wing. The flight tests successfully demonstrated the flight-worthiness of the variable geometry control surfaces. We provide an overview of structural and systems design requirements, test flight envelope (including critical design and test points), results from structural fatigue and acoustic testing, and CFD estimates on drag reduction. We also include a CFD-based aerostructural shape optimization study to evaluate the application of this technology to a twin-aisle commercial aircraft.

1 Introduction

The U.S Air Force and NASA concluded a series of flight tests on a Gulfstream III business jet retrofitted with shape adaptive trailing edge control surfaces under a program called Adaptive Compliant Trailing Edge (ACTE) [10, 4] [1]. The long-sought goal of practical, seamless, shape-changing control surface technologies has been realized by the ACTE program in which the high-lift flaps of the Gulfstream III test aircraft were replaced by a 19-foot spanwise FlexFoil™ variable-geometry control surfaces on each wing, including a 2 ft wide compliant fairings at each end, developed by FlexSys Inc. The flight tests successfully demonstrated the flight-worthiness of the variable geometry control surfaces.

Modern aircraft wings and engines have reached near-peak levels of efficiency, making further improvements exceedingly difficult. The next frontier in improving aircraft efficiency is to change the shape of the aircraft wing in-flight to maximize performance under all operating conditions. Modern aircraft wing design is a compromise between several constraints and flight conditions with best performance occurring very rarely or purely by chance. Several studies have also shown the benefits of a seamless variable camber wing to optimize the performance across various flight conditions and over a range of lift coefficients [13]. The cited benefits include increases in lift to drag ratio and better performance throughout the flight envelope, resulting in fuel savings and improvements in maneuverability as well as operational flexibility. Earlier attempts by the U.S. Air Force, via its Mission Adaptive Wing (MAW) technology in the 80s, demonstrated the aerodynamic gains of morphing, but these were negated by increases in structural weight, power, and complexity of the mechanisms and actuators needed [12, 9]. Like-

[1] https://www.nasa.gov/centers/armstrong/feature/ACTE_30_percent_less_noise.html

wise, other attempts by researchers to achieve the same goal through use of "smart materials" suffered from similar weight and power penalties and also lacked scalability. The key innovation that enabled the FlexFoil™ ACTE design to reach this goal is through exploitation of natural elasticity of materials to create flexible structures that can bend and twist with uncompromising strength [11]. This new design paradigm combines the principles of computational mechanics and kinematics, and was based on initial basic research conducted at the University of Michigan and 15 years of structural, wind tunnel, and flight-testing conducted by FlexSys under Air Force SBIR Phase II and III programs. The ACTE is envisioned as a multifunctional aerodynamic surface [3] that enables (1) airfoil shape to be optimized for minimum drag over a broad range of flight conditions including large deflections for use in high lift conditions and cruise trim (2) actuation at high enough rates to enable load alleviation during maneuvers and gusts, leading to lighter weight wing structures (3) spanwise twist to achieve optimal distributions and reduce induced drag.

Fig. 1 High-lift flaps of a Gulfstream III business jet (NASA–Air Force test aircraft) were replaced with 19 ft multi-functional variable geometry control surfaces on each wing, including 2 ft wide transition surfaces.

A shape-changing airfoil is required to support large air-loads while simultaneously adapting to different operating conditions. That is, the design has to be both flexible and strong. Flexibility and strength are usually considered antithetical in conventional engineering design where strength is usually achieved through rigidity. The success of the FlexFoil™ shape changing control surface is directly related to the underlying method of compliant design[8] of kinematic structures (or joint-less mechanisms) with distributed compliance. The compliant design method exploits the natural elasticity of common materials, such as aluminum, steel, titanium, and composites. By combining the principles of continuum mechanics and kinematics, we developed algorithms for optimal arrangement of material (skeletal configuration without joints) with built-in mechanical advantage that enables desired shape changes in a controlled fashion while supporting significant external aerodynamic loads. Each section of the compliant structural system shares the load more or less equally and undergoes the specified deformation without local stress concentrations. The goal is to distribute the strain energy more or less equally, while actively morphing the surface to desired contours and supporting the external air loads. This distributed compliance enables large deformations with low stresses so that the system can be designed for high fatigue life.

2 FlexFoil Adaptive Complaint Trailing Edge (ACTE)

As a part of Air Force SBIR Phase III program, the Air Force Research Laboratory (AFRL) procured a Gulfstream III aircraft for flight-testing FlexFoil™ variable geometry control surfaces. AFRL and FlexSys teamed up with NASA's Environmentally Responsible Aviation (ERA) program in 2009. Engineers at NASA's Armstrong Flight Research Center have successfully modified and instrumented the Gulfstream III and conducted a series of flight tests between November 2014 and April 2015. The test aircraft was named the SubsoniC Research Aircraft Testbed

(SCRAT). During Phase II of testing (ACTE II), NASA extended the flight envelope up to $M = 0.85$, twisted the controls surfaces spanwise, and conducted numerous acoustic flight tests. The primary trailing edge wing flaps on the Gulfstream III were replaced with 19 ft spanwise FlexFoil™ aircraft control surfaces on each wing, including 2 ft wide compliant fairings at each end. The FlexFoil™ surface's internal mechanism had no joints to wear out, and the profile was crafted directly to the fixed portion of the wing. The shape morphing design distributes compliance throughout the structure, changing the wing camber from −9 to +40° on demand, as well as being able to twist spanwise along the trailing edge at up to 30 deg/second for gust-load alleviation. The control surfaces are able to generate over 11,500 lbs of lift and yet maintain their unique flexibility. The surfaces are also rugged, able to withstand −650F to 1800F, harsh chemicals, and tested without failure to last five times the life cycles of a commercial aircraft. Because of its underlying mechanics, the FlexFoil™ control surface can be twisted spanwise along its length, to tailor spanwise lift distribution. This capability offers two additional benefits: (1) shifting aerodynamic loads closer to the wing root thereby reducing wing stresses, hence allowing for lighter wing structures and additional fuel savings, and (2) reducing induced drag saving even more fuel. Although Airbus A350 and Boeing 787 already tailor the spanwise lift distribution using ailerons and flaps to reduce induced drag during cruise, FlexFoil™ control surfaces offer a more refined and smooth spanwise variation due to it ability to morph (chordwise and spanwise) seamless surfaces.

2.1 Design Loads and Validation

Based on CFD analysis using TRANAIR and Star-CCM CFD codes on full 3D aircraft geometry at various flap positions and flight configurations, a comprehensive list of lift and hinge-moments was generated by NASA (Fig. 2). The resulting load-limit cases were used to design the FlexFoil™ ACTE system. Figure **??** shows the aircraft flight envelope, where the red dots correspond to the design limit load cases for which the ACTE system was designed and validated through physical testing.

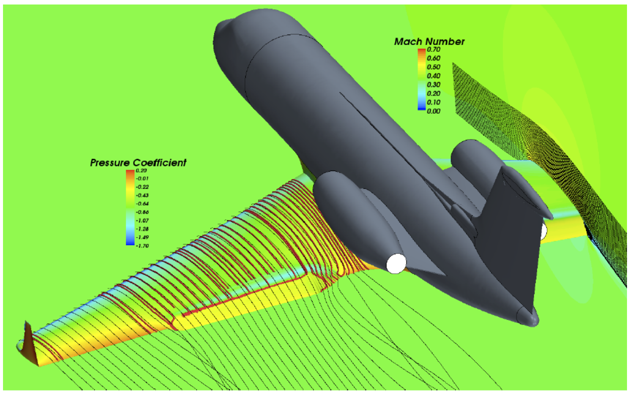

Fig. 2 Design loads were derived via Tranair and Star-CCM+ CFD codes.

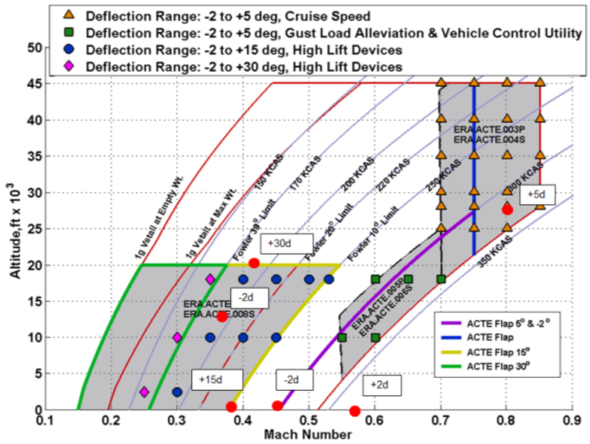

Fig. 3 Gulfstream III flight envelope and final design limit load cases used for ACTE system design (red dots).

2.2 Structural Tests and Model Validations

A building block approach was adopted in sequentially validating, through material characterization, computational analysis and physical testing, every component, sub-assembly and final assembly of the ACTE flight articles. This enabled us to gain insights and identify potential failures early in the design and development process to avoid delays and cost increases. Nonlinear finite element models of the flight article were developed incorporating material characterization test data and validated with data from structural tests conducted on various components and subassemblies. Operational tests showed that the actuation force and strain gauge measurements were, on average, within 8% of the values predicted from the model. The tests proved the model accurately predicted the shape of the morphed control surfaces. The external load tests proved that the flight articles could handle at least the aerodynamic loads with a 50% margin, and all the tested coupons survived at least 2.18 times the design limit load. On average, the actuation force was within 9% of the model predictions, and the strains were within 10% of the model predictions. Fatigue tests validated the composite material's S-N curve and ensured the reliability of the flight articles for all flight tests. Fatigue tests on all shape adaptive control surfaces were successfully carried out, exceeding the 80,000 cycles of high lift deployment (-2° to $+30^\circ$ camber change) and 500,000 cycles of deflections needed for cruise trim and gust-load alleviation.

A ground vibrations test (GVT) was conducted on the right section of the flight article with shape-adaptive trailing edge control surface along with the two transition surfaces (compliant fairings). This "free-free" GVT was conducted at NASA, for the purpose of validating analytical models. These dynamic tests are critical because they identify structural dynamic behaviors that could be excited in flight. Detailed analysis confirmed that the ACTE system has little impact on the flutter characteristics and that the flutter margin is significant and of no concern.

2.3 Weight and Power

The 19 ft FlexFoil$^{\text{TM}}$ ACTE flap weighs approximately 4% more than the weight of the baseline Gulfstream III flaps and tracks that it replaced. However, retrofitting the ACTE system involved use of miscellaneous hardware for adaptation into existing wing structure, which would not be needed in a clean sheet design. The flight article does not have any actuators, and therefore there is no in-flight actuation of the ACTE control surfaces. However, the ground article (the Iron Wing) was equipped with oversized industrial off-the-shelf actuators (weighing 110 lbs.) operating at much lower hydraulic pressure. The use of higher-pressure aerospace-grade actuators would reduce the size, and hence the weight, of the actuators needed. Using certifiable aerospace-grade actuators, the weight penalty of FlexFoil$^{\text{TM}}$ control surfaces would likely be less than 10%.

The power required to driving the ACTE control surface at similar rate as a conventional flap is comparable to a conventional flap. Depending on the application, the power required to drive FlexFoil$^{\text{TM}}$ control surfaces will be 10–20% more compared to conventional hinged flaps. However, the power required for gust load alleviation is significantly higher. The ACTE system is capable of spanwise twist of 5° at rates of 300° per second.

3 Flight Testing on the Gulfstream III

The procedure for flight-testing included Tech Briefs by NASA, which were grouped by test type (taxi or flight) and flap deflection. In total, there were five Tech Briefs conducted through the flight phase. Figure 4 shows the flight card procedure within a flight: increase in altitude with minimal increase in dynamic pressure, followed by increases in dynamic pressure at higher altitudes and as the vehicle descends at higher Mach numbers.

In accordance with NASA safety requirements, a chase aircraft accompanied the test aircraft for all flights. Table 1 lists 24 flight tests from the first phase (over 70 total) that were conducted, including the maximum altitude and dynamic pressure cleared with each flight.

During each flight, specific maneuvers were used to generate different types of data for each discipline. The configuration of these maneuvers was such that aircraft controllability, airworthiness, and high load conditions were generated from their compilation.

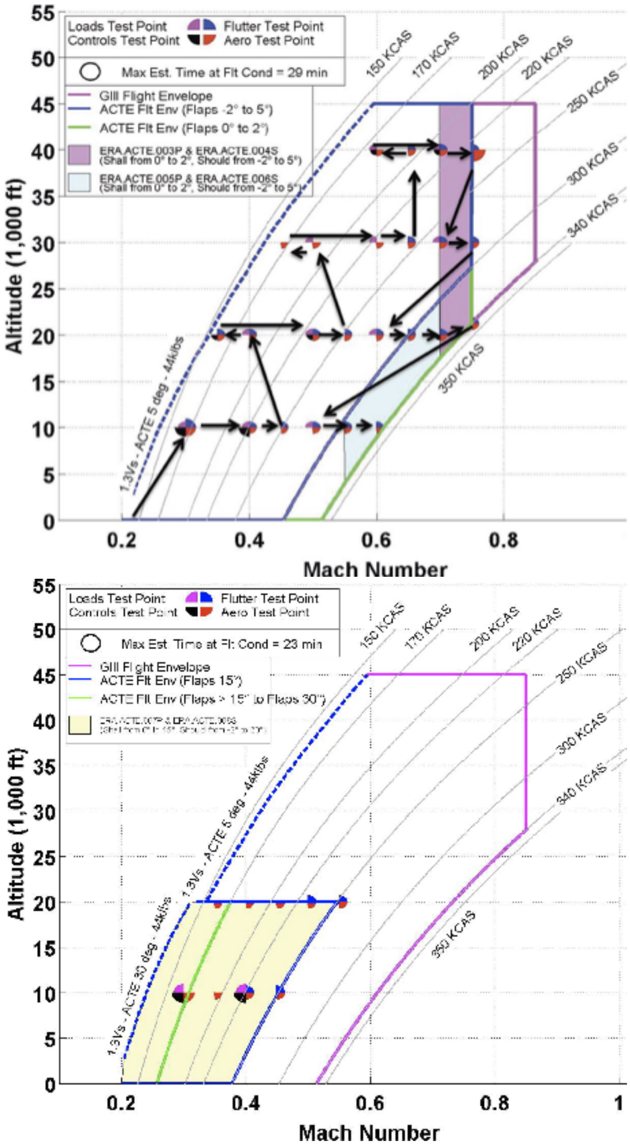

Fig. 4 Flight test procedure for stepping through test points; (top) −2 to +5 degrees and (bottom) +15 to +30 deg.

3.1 Instrumentation

The ACTE system and the test aircraft were fully instrumented to obtain data from over 5800 sensors in order to monitor structural performance and aerodynamic data to validate loads and flight conditions. The sensor array included accelerometers, fiber optic strain sensors (FOSS), hot films, pressure sensors, strain gages, and thermocouples. Nearly 1200 of these sensors were incorporated during baseline flights (SCRAT 0B) and remained on the unmodified-side of the aircraft.

Flap Setting	Cleared Alt. (ft)	Max Q (psf)	Max Accel (Gs)
20	High Speed Taxi	NA	NA
0	10,000	206	1.7
0	20,000	206	1.7
0	40,000	310	1.85
0	40,000	384	1.8
2	20,000	215	1.74
2	40,000	213	1.91
2	40,000	370	1.8
5	30,000	210	1.7
10	20,000	210	1.8
12.5	20,000	210	1.96
15	20,000	206	1.8
17.5	20,000	100	1.7
20	20,000	100	1.7
25	20,000	100	1.7
5	40,000	200	1.8
5	40,000	304	1.97
-2	20,000	206	1.7
-2	40,000	206	1.7
-2	40,000	245	1.7
-2	40,000	300	1.7
30	20,000	101	1.7
15	20,000	200	1.7

Table 1 Overview of ACTE flights conducted by NASA.

The ACTE system alone was instrumented to gather over 4300 FOSS data points, 112 strain gages, 60 accelerometers and hot film sensors (Fig. 5). Data from these sensors were used to monitor loads in real-time and also provide post-processed views of the distributed structural strains under load. Particular loads being monitored include hinge-line shear and bending loads (flap lift and hinge-moment) and actuation force (load on ACTE structure).

3.2 Structural and Aerodynamic Data

While some of the aerodynamic data was evaluated during flights, the primary objective was to validate loads and flight conditions for the ACTE system. Pressure data was acquired on the upper and lower surfaces via strip-a-tube. The flap mid-span section had electronic tufts for monitoring flow separation. A hot film sensory array on the leading edge measured the stagnation point (Fig. 6).

ACTE Structures Flight Summary										
ACTE Setting	Test Point	Flight Date	Flight #	Mach	Dynamic Pressure, psf	Altitude, ft	Flap Normal Force, lb	Flap Bending Moment, in-lb	All Flight Points	
-2	Anchor	3/31/2015	32	0.30	94	10,000	248	-2000	Max QBAR (psf):	290
-2	Anchor	3/31/2015	32	0.40	162	10,000	-5	4771	Max Nz (Gs):	1.7
-2	Anchor	4/15/2015	35	0.50	256	10,000	-310	14831		
-2	Max QBAR	4/15/2015	35	0.65	284	20,000	-358	19885		
0	Anchor	12/9/2014	18	0.30	94	10,000	419	-10197	Max QBAR (psf):	384
0	Anchor	11/6/2014	15	0.40	161	10,000	609	-13096	Max Nz (Gs):	1.8
0	Anchor	12/9/2014	18	0.50	261	10,000	639	-14828		
0	Max Mach	12/9/2014	18	0.75	354	21,200	931	-19498		
0	Max QBAR	12/9/2014	18	0.60	371	10,000	600	-17402		
2	Anchor	12/18/2014	20	0.30	92	10,000	1216	-19630	Max QBAR (psf):	372
2	Anchor	12/15/2014	19	0.40	163	10,000	1561	-29728	Max Nz (Gs):	1.8
2	Anchor	1/13/2015	21	0.50	255	10,000	1997	-44686		
2	Max Mach	1/13/2015	21	0.75	354	21,200	2989	-68120		
2	Max QBAR	1/13/2015	21	0.60	366	10,000	2474	-62182		
5	Anchor	1/22/2015	23	0.30	92	10,000	1807	-33432	Max QBAR (psf):	305
5	Anchor	3/25/2015	31	0.40	174	10,000	2503	-52777	Max Nz (Gs):	2.0
5	Anchor	3/25/2015	31	0.50	246	10,000	3168	-72994		
5	Max Mach	3/25/2015	31	0.75	240	30,000	4157	-82584		
5	Max QBAR	3/25/2015	31	0.65	287	20,000	4127	-87678		
10	Anchor	2/4/2015	24	0.30	91	10,000	2652	-51991	Max QBAR (psf):	210
10	Anchor	2/4/2015	24	0.40	167	10,000	4134	-88845	Max Nz (Gs):	1.8
10	Max Mach/QBAR	2/4/2015	24	0.55	200	20,000	5246	-111194		
12.5	Anchor	2/11/2015	25	0.40	162	10,000	4760	-102714	Max QBAR (psf):	208
12.5	Max Mach/QBAR	2/11/2015	25	0.55	198	20,000	6056	-129118	Max Nz (Gs):	2.0
15	Anchor	2/18/2015	26	0.30	90	10,000	3362	-67375	Max QBAR (psf):	210
15	Anchor	2/18/2015	26	0.40	169	10,000	5672	-120802	Max Nz (Gs):	1.7
15	Max Mach/QBAR	2/18/2015	26	0.55	200	20,000	6883	-145069		
17.5	Anchor	2/24/2015	27	0.30	92	10,000	3723	-75262	Max QBAR (psf):	110
17.5	Max Mach/QBAR	2/24/2015	27	0.38	95	20,000	3952	-78355	Max Nz (Gs):	1.7
20	Anchor	3/3/2015	28	0.30	90	10,000	3920	-79019	Max QBAR (psf):	103
20	Max Mach/QBAR	3/3/2015	28	0.38	94	20,000	4172	-82810	Max Nz (Gs):	1.7
25	Anchor	3/12/2015	29	0.30	94	10,000	4183	-83375	Max QBAR (psf):	100
25	Max Mach/QBAR	3/12/2015	29	0.38	95	20,000	4432	-88067	Max Nz (Gs):	1.8
30	Anchor	4/22/2015	36	0.30	93	10,000	4451	-88907	Max QBAR (psf):	101
30	Max Mach/QBAR	4/22/2015	36	0.38	95	20,000	4744	-93781	Max Nz (Gs):	1.7

Table 2 Summary of the flights that resulted in notable load cases.

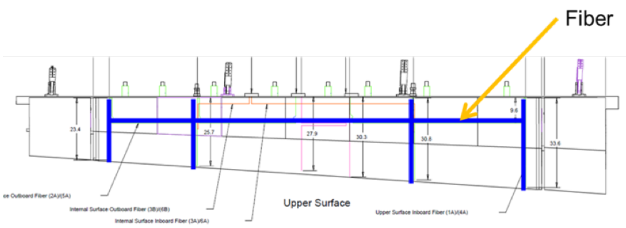

Fig. 5 Structural health monitoring with fiber optic sensors and strain gauges on ACTE system.

Figure 7 show aerodynamic coefficients of lift and moment variations as functions of flap angle and Mach number. This data shows increase in lift and moment with increase in "flap angle" or deflection of the variable geometry control surface. However, the slope of the lift curve decreases slightly beyond 15° of flap deflection, highlighting onset of flow separation. The aerodynamic model using Cmarc panel code and TRANAIR code produced identical results for flap positions up to 15°, where flow separation was observed. The flow separation at flap positions above 15° suggests the need to use of a full Navier–Stokes CFD code [14] in the future to minimize discrepancies between experimental (flight) data and model predictions.

3.3 Noise Reduction

In 2017, NASA's Langley Research Center in Virginia conducted a series of flight tests on

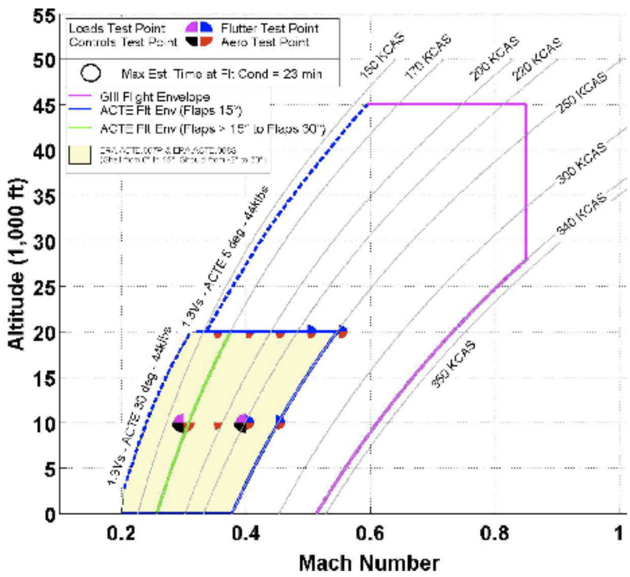

Fig. 6 The left wing was instrumented with an extensive suite of aerodynamic sensors, including pressure ports, dynamic pressure sensors, electronic tufts, and hot film sensors.

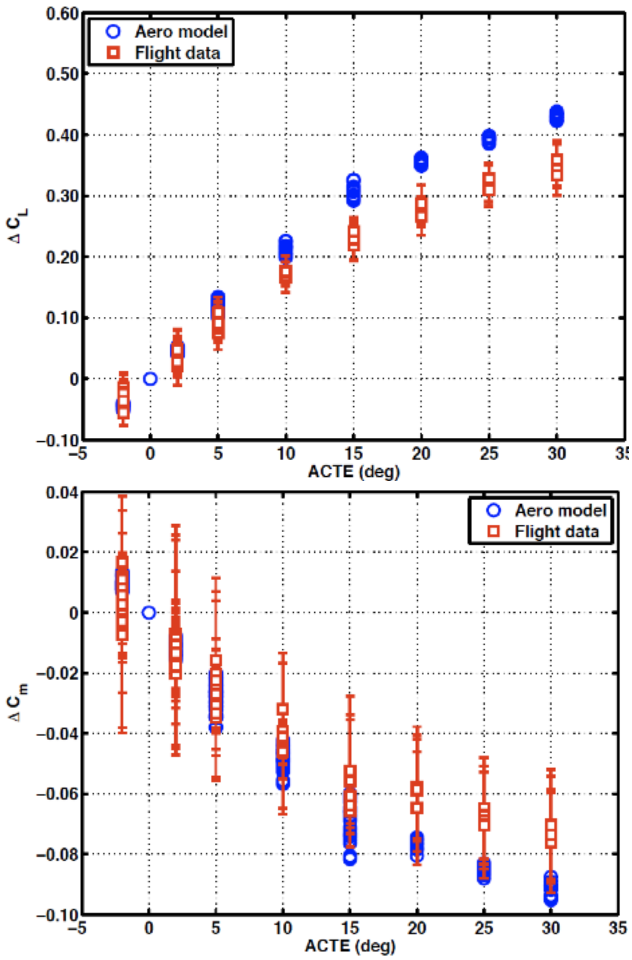

Fig. 7 Delta C_l and C_m versus flap deflection.

Gulfstream III aircraft: a baseline configuration and another one with ACTE. The a microphone array with 185 hardened microphones was arranged in a pattern of 12 spiral arms on the Rogers Dry Lakebed. This acoustic array was designed to identify those components of the aircraft that produce the highest levels of airframe noise, including elements that are deployed during the aircraft's approach and landing, such as the wing flaps, main landing gear, and nose landing gear. Additionally, four certification microphones were installed around the perimeter of the array to measure the total amount of noise the aircraft makes as it flies over. Researchers compared data collected from the baseline Gulfstream III aircraft with the ACTE configuration to calculate the exact amount of total noise reduction resulting from ACTE technology. These sets of data will help NASA closely follow guidelines for certification by the Federal Aviation Administration. NASA reported that ACTE can reduce aircraft noise by as much as 30 percent on take-off and landing[2]. Details of the test results will be released in the near future.

4 Optimization of an Airliner with ACTE

To evaluate the potential benefits on both the aerodynamic and structural performance of a commercial transport aircraft, we now present the aerostructural design optimization of a twin-aisle airliner, represented by the undeflected Common Research Model (uCRM) [1]. In this section, we merely summarize the approach and results. A much more detailed description of the approach can be found in previously published work [7, 6, 5]. More results and insights on the

[2]`https://www.nasa.gov/centers/armstrong/feature/ACTE_30_percent_less_noise.html`

benefits of morphing this configuration can be found in our previous work [2].

The aerodynamics are modeled using Reynolds-averaged Navier–Stokes CFD, while the structures is analyzed using a detailed finite-element structural model of the wing. The aerodynamics and structures are coupled to compute the wing deflections and performance at the given flight conditions.

The first step in this study is the definition of a non-morphed baseline wing design. We obtain this baseline by performing a multipoint aerostructural optimization where we optimize structural sizing and aerodynamic shape variables simultaneously to minimize the fuel burn. Angle of attack and tail rotation design variables are included for each flight condition. The baseline shape of the wing at the nominal flight condition is defined with 192 shape variables and 8 twist variables. 854 structural variables including panel thicknesses, panel lengths, stiffener heights, stiffener thicknesses, and stiffener pitches control the wing box definition. 32 morphing variables are added for each non-nominal flight condition to control the shape of the trailing 10% of the wing.

The lift and pitching moment are constrained at each flight condition. The geometric volume of the wing cannot be decreased, to provide space for fuel in the wing. Geometric thickness constraints provide low speed performance, manufacturability, and sufficient space for actuators at the leading edge, trailing edge, and aft spar, respectively. Linear shape constraints prevent shearing twist and maintain constant thickness in the morphing region. The failure of all structural members at the pull up condition are aggregated. The buckling of all non-rib structural members is constrained at the pull up and push over conditions, with aggregated constraints. In total, the optimization problem includes 1046 constraints.

The results of the initial multipoint optimization are shown in Fig. 8. Note that this multipoint optimization was run twice, once with morphing and a second time without morphing, for comparison. The non-morphing optimized wing is shown on the left of Figure 8, while the morphing result is to the right. The green lines correspond to the non-morphing case and blue lines are for the morphing configuration. Additionally, the solid lines represent the nominal cruise condition, while the dashed lines are for the 2.5g maneuver.

The morphing wing reduced the average fuel burn by 2.05% compared with the non-morphing optimized wing. This fuel burn reduction is largely enabled by the 12.4% reduction in wing mass provided by active load alleviation at maneuver. As shown in the airfoil slice data of Fig. 8, this mass reduction is provided by reflex camber in the outboard regions of the wing during the 2.5g maneuver. The effects of the reflex camber can be seen in the corresponding pressure distributions (for maneuver, on slices C and D), where regions of negative lift are produced near the trailing edge. This morphing shifts the maneuver load inboard, enabling the lighter structure shown in the thickness distributions. That lighter structure is more flexible than its heavier counterpart in the non-morphing wing, which produces some aerodynamic penalties, but the optimizer balances those competing effects, and produces the optimal design.

5 Conclusions and Future Work

The primary purpose of the flight tests carried out by NASA and AFRL was to demonstrate the structural feasibility and robustness of the FlexFoil^{TM} ACTE technology. The FlexFoil^{TM} variable geometry technology on the experimental Gulfstream III aircraft was not optimized for maximum aerodynamic load benefit, but future clean sheet optimized designs will tailor the structure for maximum aerodynamic load advantage. For instance, using multidisciplinary design optimization codes to perform RANS-based aerodynamic analysis/shape optimization for various combinations of Mach-C_L and construct the drag polar of the morphing FlexFoil^{TM}, allows us to identify trailing edge shapes that yield minimum drag throughout the flight profile [14]. The variable geometry control surfaces on all the flight tests worked flawlessly. The test aircraft fit-

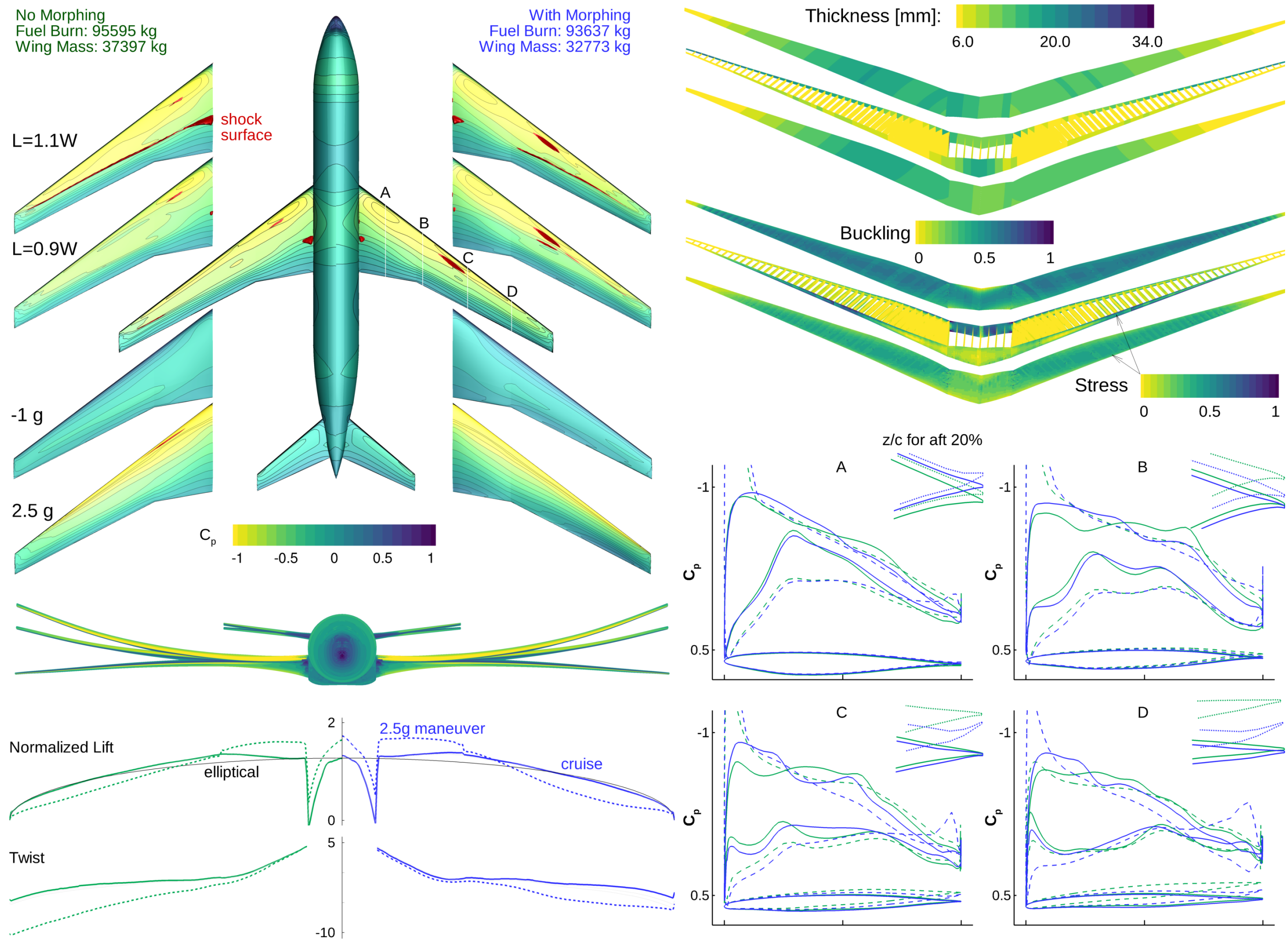

Fig. 8 Comparison of the aerostructural multipoint optimization results with and without a morphing trailing edge on the aft 10% of the wing. The maneuver load alleviation enabled by the morphing trailing edge leads to a 12.4% reduction in the wing mass and a 2.72% reduction in the average fuel burn.

ted with ACTE control surfaces was flown in the initial phase at $M = 0.75$, at a maximum altitude of 40,000 ft and was subjected to 2g maneuvers and a maximum dynamic pressure of 384 psf. Overall, the ACTE structure survived the rigors of over 70 hours of flight tests without any structural failures a loads exceeding the maximum design loads for commercial aircraft.

During the second phase of flight tests, through a new program entitled Flight Demonstrations and Capabilities (FDC), NASA successfully completed a series of flight tests at $M = 0.85$. Additional flight tests were carried out with control surfaces subjected to a spanwise of $\pm 5°$ to assess the shift in center of lift. A series of acoustic flight tests were also carried out NASA Langley. NASA reported that ACTE can reduce aircraft noise by as much as 30 percent on takeoff and landing.

As anticipated, a seamless trailing edge surface, such as FlexFoil™ ACTE, experiences loss of high-lift capability at low speeds due to (1) absence of slots to direct high pressure air over Fowler/hinged flap and (2) lack of increase in wing area afforded by a conventional flap. Therefore, flow augmentation devices for maintaining flow attachment at flap positions above 15° are needed to attain lift closer to that generated by conventional flaps. Active flow control methods, such as “blown slot” with sweeping jets, successfully tested under another NASA ERA program, are capable of adding momentum to the flow on the airfoil upper surface, thereby keeping the boundary layer attached over highly-deflected surfaces of ACTE. uch flow augmentation methods will be explored in the future. Having demonstrated the structural feasibility and robustness of shape adaptive seamless control surfaces through a series of rigorous and successful flight tests, several applications of FlexFoil™ variable geometry technology will be explored in the near future for other control surfaces including trailing edge trim tabs, leading edge, engine inlets, winglets, stabilizers, rudders and ailerons.

The numerical design optimization study in this article considered a clean sheet redesign of a twin-aisle commercial transport aircraft with a small morphing trailing edge device. The clean sheet configuration was designed with an aerostructural multipoint optimization. This optimization included morphing capabilities and structural sizing design variables, and thus took advantage of the active load alleviation enabled by the morphing trailing edge. Compared with a clean sheet design optimized without a morphing trailing edge, the weight of the ACTE wing is 12.4% lower. The multipoint optimized morphing wing was used as the baseline for 65 aerostructural morphing shape optimizations. The optimized performance of the morphing wing at a variety of flight conditions was aggregated into a performance surrogate that was used for mission analysis. Over the course of a full mission, the clean sheet morphing design required 2.72% less fuel than the baseline.

Acknowledgements

The first author would like to thank (1) the AFRL at Wright Patterson Air Force base for their vision, guidance, and funding support (Air Force SBIR Phases I, II and III) over the past 14 years to validate and test the FlexFoil™ variable geometry technology and (2) NASA ERA for its funding the flight test program and NASA AFRC engineers for instrumenting the wing and conducting flight tests. The second author would like to thank Fay Collier, who supported the design optimization effort through NASA award number NNX14AC73A.

References

[1] T. R. Brooks, G. K. W. Kenway, and J. R. R. A. Martins. Benchmark aerostructural models for the study of transonic aircraft wings. *AIAA Journal*, 2018. (In press).

[2] D. A. Burdette, G. K. W. Kenway, and J. R. R. A. Martins. Aerostructural design optimization of a continuous morphing trailing edge aircraft for improved mission performance. In *17th AIAA/ISSMO Multidisciplinary Analysis and Optimization Conference*, Washington, D.C., June 2016.

[3] G. Gilyard and M. Espana. On the use of controls for subsonic transport performance improvement: Overview and future directions. Technical Memorandum 4605, NASA Dryden Flight Research Center, 1994.

[4] J. A. Hetrick, R. F. Osborn, S. Kota, P. M. Flick, and D. B. Paul. Flight testing of mission adaptive compliant wing. In *Proceedings of the 48th AIAA/ASME/ASCE/AHS/ASC Structures, Structural Dynamics, and Materials Conference*, Honolulu, HI, April 2007. AIAA 2007-1709.

[5] G. K. W. Kenway, G. J. Kennedy, and J. R. R. A. Martins. Scalable parallel approach for high-fidelity steady-state aeroelastic analysis and derivative computations. *AIAA Journal*, 52(5):935–951, May 2014.

[6] G. K. W. Kenway and J. R. R. A. Martins. Multipoint high-fidelity aerostructural optimization of a transport aircraft configuration. *Journal of Aircraft*, 51(1):144–160, January 2014.

[7] G. K. W. Kenway and J. R. R. A. Martins. Buffet onset constraint formulation for aerodynamic shape optimization. *AIAA Journal*, 55(6):1930–1947, June 2017.

[8] S. Kota. System for varying a surface contour. Technical report, U.S. Patent Office, 1999. U.S. Patent No. 5,971,328.

[9] S. Kota. Shape-shifting things to come. *Scientific American*, pages 58–65, May 2014.

[10] S. Kota, P. Flick, and F. S. Collier. Flight testing

of flexfloil adaptive compliant trailing edge. In *54th AIAA Aerospace Sciences Meeting, AIAA SciTech Forum*, San Diego, CA, January 2016.

[11] S. Kota, J. Hetrick, R. Osborn, D. Paul, E. Pendleton, P. Flick, and C. Tilmann. Design and application of compliant mechanisms for morphing aircraft structures. In *Proceedings of the SPIE Smart Structures and Materials Conference*, San Diego, CA, March 2003.

[12] S. Kota, R. Osborn, G. Ervin, D. Maric, P. Flick, and D. Paul. Mission adaptive compliant wing—design, fabrication and flight test. Technical Report RTO-MP-AVT-168, NATO Research and Technology Organization, 2007.

[13] J. R. R. A. Martins. *Encyclopedia of Aerospace Engineering*, volume Green Aviation, chapter Fuel burn reduction through wing morphing, pages 75–79. Wiley, October 2016.

[14] E. Miller, J. Cruz, S.-F. Lung, S. Kota, G. Ervin, K.-J. Lu, and P. Flick. Evaluation of the hinge moment and normal force aerodynamic loads from a seamless adaptive compliant trailing edge flap in flight. In *Proceedings of the AIAA Science and Technology Forum and Exposition (SciTech)*, San Diego, CA, 2016.

6 Contact Author Email Address

mailto: kota@umich.edu

Copyright Statement